Applied Physics Express 12, 112003 (2019) LETTER
https://doi.org/10.7567/1882-0786/ab4b35

Interfacial charge transfer between $CsPbBr_3$ quantum dots and ITO nanoparticles revealed by single-dot photoluminescence spectroscopy

Bin Li[1,2], Ruiyun Chen[1,2], Chengbing Qin[1,2], Changgang Yang[1,2], Wenli Guo[1,2], Xue Han[1,2], Yan Gao[1,2], Guofeng Zhang[1,2*], Liantuan Xiao[1,2*], and Suotang Jia[1,2]

[1]State Key Laboratory of Quantum Optics and Quantum Optics Devices, Institute of Laser Spectroscopy, Shanxi University, Taiyuan, 030006, People's Republic of China
[2]Collaborative Innovation Center of Extreme Optics, Shanxi University, Taiyuan, 030006, People's Republic of China

*E-mail: guofeng.zhang@sxu.edu.cn; xlt@sxu.edu.cn

Received August 23, 2019; revised September 23, 2019; accepted October 4, 2019; published online October 16, 2019

The interfacial charge transfer between single $CsPbBr_3$ perovskite quantum dots (QDs) and indium tin oxide (ITO) is investigated by single-dot photoluminescence spectroscopy. It is found that when the Fermi level of single perovskite QDs aligns with that of ITO nanoparticles, the QD surface cannot be charged by the ITO through interfacial electron transfer. Therefore, the QD/ITO system with Fermi level alignments can exclude exciton nonradiative recombination processes involving the additional surface electrons, such as the exciton Auger recombination and the valence band hole transfer processes. Hence the photovoltaic devices based on perovskite QD/ITO system with the Fermi level alignments have the improved photoelectric conversion efficiency. © 2019 The Japan Society of Applied Physics

Supplementary material for this article is available online

Lead halide perovskites have attracted great attention in a wide variety of applications such as solar cells, light-emitting devices (LEDs) and lasers because of their attractive optical and electronic properties as well as low cost and solution processability.[1–3] Among them, high-quality all-inorganic $CsPbX_3$ (X = Cl, Br or I) perovskite quantum dots (QDs) prepared by the colloidal synthesis method, exhibit excellent optical properties such as high photoluminescence (PL) quantum yields and adjustable band gap covering the entire visible spectrum.[4–6] Besides, perovskite QDs also have a "soft" and predominantly ionic lattice and their optical and electronic properties are highly tolerant to structural defects and surface states.[7,8] Recently, effective LED and low-threshold lasers have been developed based on all-inorganic perovskite QDs.[9,10] In particular, the photoelectric conversion efficiency (PCE) of perovskite solar cells has been largely enhanced from 3%–4% in 2009[11] to ~25% in recent years.[12]

When fabricating perovskite photovoltaic devices, the method of directly preparing the perovskite material onto a transparent conductive oxide electrode (or metal electrode) instead of the transport layer can reduce the complexity and cost of industrial manufacturing. The PCEs of 10.49%[13] and 10.85%[14] can be achieved respectively by the Au/perovskite junctions without using the hole transport layer. While perovskite material directly contacts with indium tin oxide (ITO), such as inverted ITO/perovskite/C60/BCP/Ag structure, the maximum PCE can reach up to 16%.[15] By adjusting the Fermi level of perovskite material by Cu doping, it was found that when the Fermi level of perovskite material is similar to that of ITO, the PCE of ITO/Cu-perovskite/PCBM/Ag device can reach the maximum value.[16] Clearly, Fermi level alignments can influence the charge extraction, collection, and recombination kinetics, and thus affect the PCE of photovoltaic devices. However, the exact physical processes involved in the perovskite/ITO system with Fermi level alignments need to be further explored.

In this study, we investigate the interfacial charge transfer dynamics between $CsPbBr_3$ perovskite QDs and ITO nanoparticles by single-dot PL spectroscopy. The Fermi level of ITO nanoparticles has been selected to match that of $CsPbBr_3$ QDs. By a confocal scanning microscope equipped with time-tagged time-resolved time-correlated single photon counting (TTTR-TCSPC) acquisition card, PL intensity trajectories of single QDs, PL decay curves, second-order correlation functions ($g^{(2)}$) curves as well as fluorescence lifetime-intensity distribution (FLID) can be obtained. Based on these experimental data, we investigate the interfacial electron transfer (ET) between single $CsPbBr_3$ QDs and ITO nanoparticles and then to explore the exact physical processes involved in the perovskite QD/ITO system with Fermi level alignments.

The $CsPbBr_3$ perovskite QDs used in this work were synthesized by wet chemical method according to Ref. 17). Figure 1(a) shows the absorption and PL spectra of the QDs dispersed in toluene; the PL spectrum is centered at 515 nm with a full width at half-maximum (FWHM) of 20 nm. Figure 1(b) shows the transmission electron microscopy (TEM) image of QDs with an average size of ~10 nm and a reasonable monodispersity. For the single-dot measurements, QDs in toluene were spin-coated onto ITO-coated coverslips, and then the polystyrene solution in toluene was spin-coated onto QDs to form a protective film, as shown in Fig. 1(c). The details of sample preparation and experimental setup are presented in supplementary material. Single perovskite QDs were also prepared onto glass coverslips as a control experiment. Figure 1(d) shows a typical confocal scanning PL image of single $CsPbBr_3$ QDs. It is worth noting that aggregates were also observed alongside with the single QDs; therefore, the single QDs have been distinguished during the confocal scanning imaging process by a fast recognition method demonstrated in our previous literature.[18,19]

Figure 2(a) shows the PL intensity trajectories and corresponding FLIDs for single $CsPbBr_3$ QDs on glass and ITO under same excitation conditions. The PL intensity of the bright state for the single QD on ITO (8 counts ms^{-1}) is smaller than that on glass (30 counts ms^{-1}), which was speculated to be the occurrence of interfacial ET from single excited $CsPbBr_3$ QDs to ITO.[20–23] The FLIDs in Fig. 2(a) show that the PL intensities of the single $CsPbBr_3$ QDs on both the glass and ITO are linearly related to the lifetimes,

© 2019 The Japan Society of Applied Physics

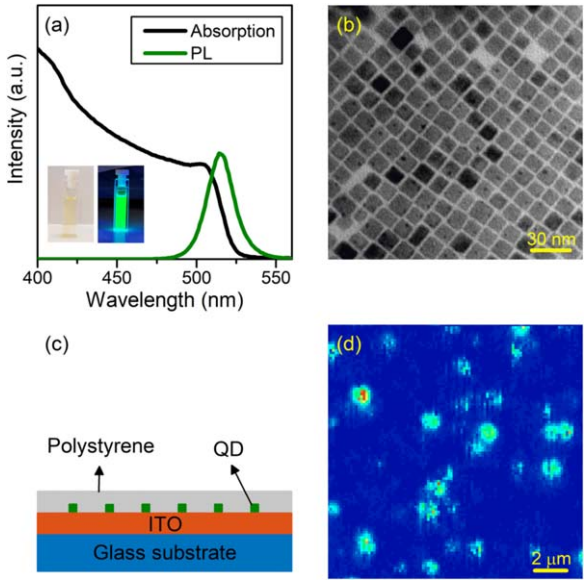

Fig. 1. (Color online) (a) Absorption and PL spectra of $CsPbBr_3$ perovskite QDs dispersed in toluene. Insets: photographs of the resultant solution under room and UV light. (b) High-resolution TEM image of QDs. (c) Schematic view of single QDs spin-coated onto an ITO nanoparticles film. The polystyrene film was used to provide protection for QDs. (d) Confocal scanning PL image of single QDs spin–coated onto ITO.

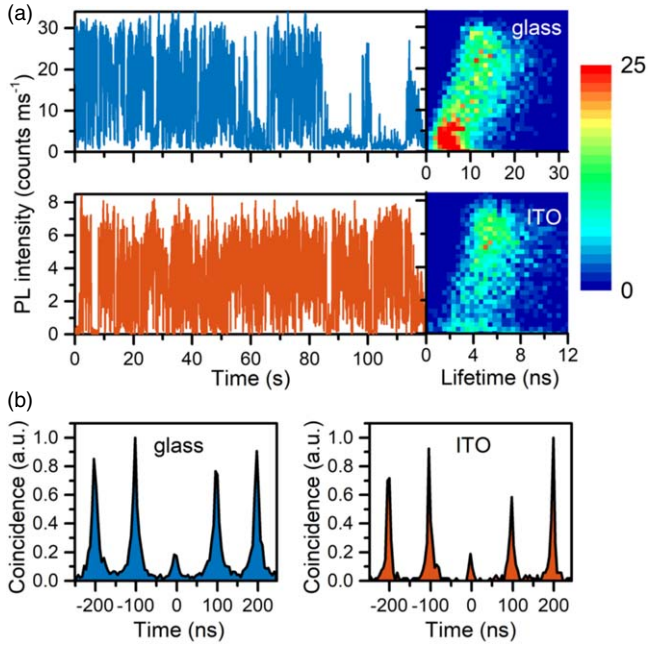

Fig. 2. (Color online) (a) Typical PL intensity trajectories for the single $CsPbBr_3$ QDs on glass and ITO substrates, respectively. The corresponding FLIDs are shown in the right panels. (b) Corresponding $g^{(2)}(\tau)$ curves.

which indicates that the PL blinking originates from the activation and deactivation of shallow surface traps.[19,24] For CdSe-based QDs, this kind of blinking can be suppressed by filling the surface traps through interfacial ET (e.g. contacting the QD with ITO).[20,21] However, FLIDs indicate that when $CsPbBr_3$ QDs are in contact with ITO, shallow surface traps are not changed by the ITO nanoparticles. This difference will be explained later according to the ET dynamics between the $CsPbBr_3$ QDs and ITO. The corresponding $g^{(2)}$ curves for the individual QDs on the glass and ITO are shown in

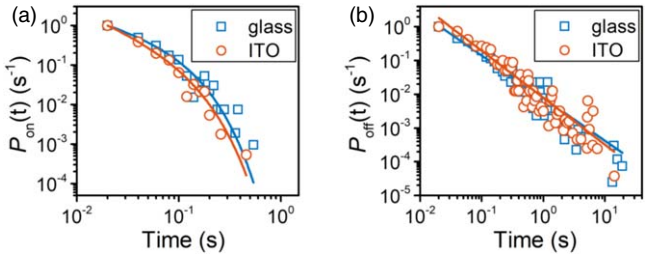

Fig. 3. (Color online) Normalized probability densities of (a) on-state [$P_{on}(t)$] and (b) off-state [$P_{off}(t)$] for single QDs on glass and ITO, respectively. The solid lines are best fits by a truncated power law for on-state and power law for off-state, respectively.

Fig. 2(b), respectively. A $g^{(2)}(0)$ value of less than 0.5 indicates that the observed PL is derived from a single QD.[18]

The PL blinking properties of single $CsPbBr_3$ QDs on glass and ITO can be quantified by probability density distribution,[25,26] as shown in Fig. 3. The on-time probability density of QDs on glass and ITO can be fitted by truncated power-law function $P_{on}(t) \propto t^{-\alpha_{on}} \exp(-t/t_c)$, while the off-time probability density can be fitted by power-law function $P_{off}(t) \propto t^{-\alpha_{off}}$, where α_{on} and α_{off} are power law exponents and t_c is the truncation time. According to the previous reports,[27] the on-time probability density of single QDs obeys the truncated power-law distribution, while the off-time probability density obeys power-law distribution. This is because the on-time probability density is sensitive to environmental conditions such as temperature, identity of surrounding matrix, pump intensity, and surface properties, while the off-time probability is virtually insensitive to these environmental conditions.[27] The distribution of on- and off-time probability density shows that the blinking behaviors of $CsPbBr_3$ QDs on ITO are almost the same as that on glass (see Table S1 in the supplementary material for statistical results, available online at stacks.iop.org/APEX/12/112003/mmedia). This phenomenon is different from CdSe-based QDs.[20,21,28] By contacting ITO nanoparticles, the PL blinking of CdSe-based QDs can be suppressed and the on-state proportion can be increased due to the interfacial ET from ITO to perovskite QDs to fill the surface traps.[20,21] In this experiment, the Fermi level of ITO nanoparticles is similar to that of perovskite QDs, so the electrons in ITO are not able to transfer onto the surface of perovskite QDs to fill in the surface traps to suppress the PL blinking. Therefore, the PL blinking of single QDs on ITO is not suppressed, indicating that the interfacial ET from ITO to single QDs does not occur.[29–31]

Although interfacial ET from ITO to perovskite QDs cannot occur due to their Fermi level alignment, photoinduced interfacial ET from single excited $CsPbBr_3$ QDs to ITO can still occur. Here, we investigate the photoinduced interfacial ET from single excited $CsPbBr_3$ QDs to ITO. PL emission of single perovskite QDs is mainly influenced by the activation and deactivation of surface traps, leading to the fluctuating non-radiative rate. Therefore, the lifetime values of single QDs fluctuate with time and the multi-exponential functions need to be used to fit the PL decay curves of single QD on glass (blue curve) and ITO (red curve) as shown in Fig. 4(a). Figure 4(b) shows histograms of the

© 2019 The Japan Society of Applied Physics

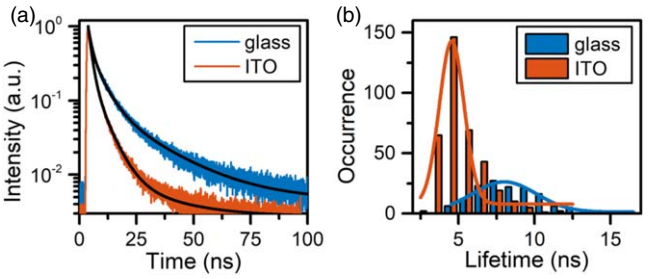

Fig. 4. (Color online) (a) PL decay curves and best exponential fits for single $CsPbBr_3$ QDs on glass and ITO, respectively. (b) Histograms of intensity-weighted average lifetimes for single QDs on glass and ITO with Gaussian fitting, respectively.

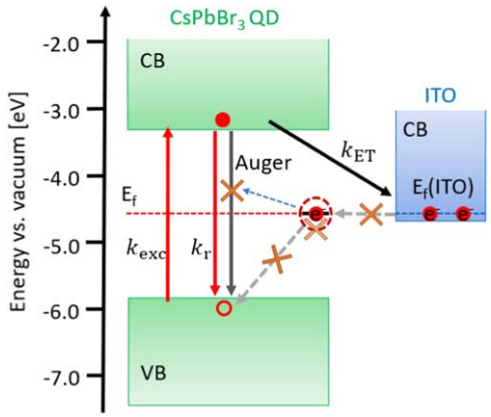

Fig. 5. (Color online) Schematic of the excitation-relaxation cycle of single $CsPbBr_3$ QD and possible ET pathways between QD and ITO. CB and VB are the conduction band and valence band, respectively; E_f is the Fermi level, k_{exc} is the excitation rate, k_r is the radiative decay rate, and k_{ET} is the rate of ET from excited QD to ITO. The grey arrow lines indicate the interfacial ET from ITO to QD and the removal of the valence band holes through the surface electron. The crosses indicate the processes that cannot occur.

intensity-weighted average lifetimes of ~150 single $CsPbBr_3$ QDs on glass and ~360 single $CsPbBr_3$ QDs on ITO. The histograms can be fitted by Gaussian functions, and the lifetime value at the Gaussian peak is 4.6 ns (8 ns) for single QDs on ITO (glass) and the FWHM is 1.9 ns (5 ns). Therefore, the lifetime values of single QDs on ITO are reduced to about 57% of that on glass. In the previous work of CdSe-based QDs, the reduced PL lifetime values were attributed to the exciton Auger recombination and the effective removal of the valence band holes involving the additional electrons on QDs' surface.[20,21] Here, because the surface of single QDs are not negatively charged by the electrons from ITO through interfacial ET, the exciton Auger recombination and the effective removal of the valence band holes through the surface electrons can be excluded. Therefore, the reduced lifetimes mainly derive from the photoinduced ET from single excited QDs to ITO. By comparing the lifetime values of single QDs on glass and ITO, the average ET rate from single $CsPbBr_3$ QDs to ITO is $9.2 \times 10^7\ s^{-1}$.

Based on the above results, we can analyze the interfacial ET dynamics between single $CsPbBr_3$ QDs and ITO and the associated physical processes involved in the perovskite QD/ITO system with Fermi level alignments. Here, we briefly recall the investigation results of the CdSe-based QDs on ITO, as reported in previous literatures.[20,21] The N-type semiconductor ITO nanoparticles have a higher Fermi level than the CdSe-based QDs. When both of them are in contact, there is a driving force for electrons to be transferred from the ITO to the CdSe-based QDs until their Fermi level reaches equilibrium, and the excess electrons on the surface of CdSe-based QDs will fill the surface traps to suppress PL blinking, as well as charge for QD surface through interfacial ET. The surface electrons of QDs induce the exciton Auger recombination and remove the valence band holes to quench exciton emission.[21] However, the single $CsPbBr_3$ QD on ITO is a different case. By referring to previous reports,[6] schematic of the excitation-relaxation cycle of single QD and possible ET pathways between QD and ITO are shown in Fig. 5. When the $CsPbBr_3$ QD is in contact with ITO, this driving force is absent due to the alignment of Fermi levels, so the electrons in ITO cannot be transferred to the perovskite QDs to charge the QD; therefore, suppression of the PL blinking was not observed for the single perovskite QDs on ITO. Besides, the QD surface is not charged, which also avoids exciton Auger recombination of the $CsPbBr_3$ QD and the effective removal of the valence band holes through the surface charges. We note, that the Fermi level of $CsPbCl_3$ and $CsPbI_3$ perovskite materials have been reported to be lower or higher than that of ITO,[6] therefore, their Fermi levels need to be adjusted to achieve the Fermi level alignments to improve the PCE of photovoltaic devices.

In conclusion, we investigated the interfacial ET dynamics and the associated physical processes involved in the perovskite QD/ITO system with the Fermi level alignments by single-dot PL spectroscopy. The FLIDs showed the existence of similar shallow surface traps of QDs in the two cases. The PL blinking of single perovskite QDs on ITO is the same as that on glass, indicating that the shallow surface traps of the QDs were not filled by the electrons of the ITO, and the QDs surface was not charged by ITO. The additional Auger recombination and the effective removal of the valence band holes involving the additional surface electrons would not happen. The reduced PL intensity and lifetime of single $CsPbBr_3$ QDs on ITO nanoparticles derived from the photoinduced interfacial ET from excited QDs and ITO. This investigation of interfacial charge transfer in perovskite QD/ITO system is helpful for understanding the improved PCE of photovoltaic devices.

Acknowledgments This research was funded by the National Key R&D Program of China (No. 2017YFA0304203), Natural Science Foundation of China (Nos. 61527824, 61675119, 61875109, 11434007, 61605104), PCSIRT (No. IRT_13076), PTIT, 1331KSC, and 111 project (Grant No. D18001).

ORCID iDs Bin Li https://orcid.org/0000-0002-5817-6792

1) B. Tang, H. X. Dong, L. X. Sun, W. H. Zheng, Q. Wang, F. F. Sun, X. W. Jiang, A. L. Pan, and L. Zhang, ACS Nano **11**, 10681 (2017).
2) E. Debroye, H. Yuan, E. Bladt, W. Baekelant, M. Van der Auweraer, J. Hofkens, S. Bals, and M. B. J. Roeffaers, ChemNanoMat **3**, 223 (2017).
3) K. I. Yuyama, M. J. Islam, K. Takahashi, T. Nakamura, and V. Biju, Angew. Chem. Int. Ed. **57**, 13424 (2018).
4) F. Zhang, H. Zhong, C. Chen, X.-G. Wu, X. Hu, H. Huang, J. Han, B. Zou, and Y. Dong, ACS Nano **9**, 4533 (2015).
5) H. Huang, L. Polavarapu, J. A. Sichert, A. S. Susha, A. S. Urban, and A. L. Rogach, NPG Asia Mater. **8**, 328 (2016).
6) V. K. Ravi, G. B. Markad, and A. Nag, ACS Energy Lett. **1**, 665 (2016).
7) H. Huang, M. I. Bodnarchuk, S. V. Kershaw, M. V. Kovalenko, and A. L. Rogach, ACS Energy Lett. **2**, 2071 (2017).

© 2019 The Japan Society of Applied Physics

8) Q. A. Akkerman, G. Raino, M. V. Kovalenko, and L. Manna, Nature Mater. **17**, 394 (2018).
9) T. Chiba, K. Hoshi, Y. J. Pu, Y. Takeda, Y. Hayashi, S. Ohisa, S. Kawata, and J. Kido, ACS Appl. Mater. Interfaces **9**, 18054 (2017).
10) S. Yakunin, L. Protesescu, F. Krieg, M. I. Bodnarchuk, G. Nedelcu, M. Humer, G. De Luca, M. Fiebig, W. Heiss, and M. V. Kovalenko, Nat. Commun. **6**, 8056 (2015).
11) A. Kojima, K. Teshima, Y. Shirai, and T. Miyasaka, J. Am. Chem. Soc. **131**, 6050 (2009).
12) F. Sahli et al., Nature Mater. **17**, 820 (2018).
13) J. J. Shi et al., Appl. Phys. Lett. **104**, 063901 (2014).
14) S. Aharon, S. Gamliel, B. El Cohen, and L. Etgar, Phys. Chem. Chem. Phys. **16**, 10512 (2014).
15) Y. L. Li, S. Y. Ye, W. H. Sun, W. B. Yan, Y. Li, Z. Q. Bian, Z. W. Liu, S. F. Wang, and C. H. Huang, J. Mater. Chem. A **3**, 18389 (2015).
16) K. Lu, Y. Lei, R. Qi, J. Liu, X. Yang, Z. Jia, R. Liu, Y. Xiang, and Z. Zheng, J. Mater. Chem. A **5**, 25211 (2017).
17) L. Protesescu, S. Yakunin, M. I. Bodnarchuk, F. Krieg, R. Caputo, C. H. Hendon, R. X. Yang, A. Walsh, and M. V. Kovalenko, Nano Lett. **15**, 3692 (2015).
18) B. Li, G. F. Zhang, C. G. Yang, Z. J. Li, R. Y. Chen, C. B. Qin, Y. Gao, H. Huang, L. T. Xiao, and S. T. Jia, Opt. Express **26**, 4674 (2018).
19) B. Li et al., J. Phys. Chem. Lett. **9**, 6934 (2018).
20) B. Li, G. F. Zhang, Z. Wang, Z. J. Li, R. Y. Chen, C. B. Qin, Y. Gao, L. T. Xiao, and S. T. Jia, Sci. Rep. **6**, 32662 (2016).
21) S. Jin, N. Song, and T. Lian, ASC Nano **4**, 1545 (2010).
22) H. Cheng, C. Yuan, J. Wang, T. Lin, J. Shen, Y. Hung, J. Tang, and F. Tseng, J. Phys. Chem. C **118**, 18126 (2014).
23) G. F. Zhang et al., Front. Phys. **14**, 23605 (2019).
24) G. Yuan, D. E. Gómez, N. Kirkwood, K. Boldt, and P. Mulvaney, ACS Nano **12**, 3397 (2018).
25) Z. Qiao, C. Qin, W. He, Y. Gong, B. Li, G. Zhang, R. Chen, Y. Gao, L. Xiao, and S. Jia, Carbon **142**, 224 (2019).
26) C. G. Yang, G. F. Zhang, L. H. Feng, B. Li, Z. J. Li, R. Y. Chen, C. B. Qin, Y. Gao, L. T. Xiao, and S. T. Jia, Opt. Express **26**, 11889 (2018).
27) J. M. Pietryga, Y. S. Park, J. H. Lim, A. F. Fidler, W. K. Bae, S. Brovelli, and V. I. Klimov, Chem. Rev. **116**, 10513 (2016).
28) Z. J. Li, G. F. Zhang, B. Li, R. Y. Chen, C. B. Qin, Y. Gao, L. T. Xiao, and S. T. Jia, Appl. Phys. Lett. **111**, 153106 (2017).
29) G. F. Zhang et al., Front. Phys. **14**, 63601 (2019).
30) H. D. Zang, P. K. Routh, Y. Huang, J. S. Chen, E. Sutter, P. Sutter, and M. Cotlet, ACS Nano **10**, 4790 (2016).
31) W. J. He, C. B. Qin, Z. X. Qiao, Y. N. Gong, X. R. Zhang, G. F. Zhang, R. Y. Chen, Y. Gao, L. T. Xiao, and S. T. Jia, Nanoscale **11**, 1236 (2019).

© 2019 The Japan Society of Applied Physics